YOUNG FLOOD LAVAS IN THE ELYSIUM REGION, MARS, J. B. Plescia, Jet Propulsion Laboratory, Pasadena, CA 91109.

The nature and origin of a smooth plains unit (the Cerberus Plains) in southeastern Elysium and western Amazonis is reported here. The Cerberus Plains cover >100,000 km^2 and extend an east-west distance of nearly 3,000 km; the plains are about 700 km wide in a north-south direction near longitude 195°. The unit is uncratered and exhibits lobate albedo patterns and embayment relations with older terrane. Morphologic characteristics suggest fluidized emplacement and the unit is interpreted to be formed by the eruption of large volumes of very low viscosity lava. A volcanic origin for this unit was also suggested by Schaber (1980), but he felt that the unit had been heavily modified by aeolian processes and he did not discuss its origin in detail. Tanaka and Scott (1986) and Tanaka (1986) reached a different conclusion and interpreted the material to be sedimentary, deposited during a fluvial episode.

The Cerberus Plains are one of the youngest units on Mars, crater numbers of 89 ±15 craters >1 km/10^6 km^2 were measured during this study. Carr and Clow (1981) cite 1 km crater numbers of <600; and Scott and Tanaka (1986) cite numbers of <50. Embayment relations indicate the Cerberus Formation overlies all other units in the Elysium region and western Amazonis (Greeley and Guest, 1987; Scott and Tanaka, 1986).

The Cerberus Plains are characterized by distinct linear albedo patterns independent of the wind streaks associated with aeolian processes. These patterns suggest an eastward flow across the Cerberus Plains, then a northeastward flow through a topographic low in the knobby terrane (exploiting a series of older channels carved into knobby terrane and ridged plains during an earlier period), and then out into Amazonis Planitia. In the east the albedo patterns are regionally organized forming bands up to 40 km wide; in the western areas, the albedo patterns are complex and intricate with high-frequency digitate boundaries varying from narrow, meandering patterns to broad, equant "ponded" shapes.

Small-scale surface texture of the plains is difficult to resolve; only in the highest resolution images are the relevant morphologic details observable. Near 19°N, 174°W the unit fills a channel cut through older plains and knobby terrane; here the channel floor appears smooth whereas the surrounding terrane has significant texture and numerous 400-600 m diameter craters. Apparently the original floor is covered by material younger than the surrounding plains. At the southern margin of the Cerberus Plains the surface shows a myriad of surface details indicative of a lava flow--pressure ridges, flow fronts, and flowage around obstacles; a festoon pattern is observed locally indicative of flowage up against the topographically higher areas. Morphology suggestive of a volcanic origin is also observed in western Amazonis Planitia (near 22°N, 170°W) where the distribution of material indicates flow and where the material terminates in a series of digitate and lobate fronts about 10 m high.

Six eruptive vents have been identified; the morphology of these features is suggestive of low shields--constructional volcanic features a few hundred meters high having lava flows emanating both as floods from a central vent and through a tube and channel system (e.g., Mauna Ulu and Mauna Iki; Greeley, 1982). Some of the Cerberus shields are elongate having elliptical vents; others are more symmetric. Summit vents range from 1-2 km diameter for circular vents; up to 15 km in length for elongate vents.

The morphology of the Cerberus Plains suggests it is an example of flood basalt volcanism; the morphology of western part indicates plains style volcanism. Terrestrial examples of flood basalts include the Deccan Traps and the Columbia Plateau (specifically the Yakima Basalt). Flood basalt provinces (Greeley, 1976, 1982) are characterized by flows 5-45 m thick extending over large areas and exhibiting little relief. Eruption rates for flood basalts are many times greater than for central volcanoes and the vents are fissure systems typically tens to hundreds of kilometers long in zones several kilometers wide. Western Cerberus Plains (near longitude 200°) appears to be a basaltic lava plains style of volcanism (e.g., the Snake River Plains of Idaho; Greeley, 1976, 1982). Plains volcanism is characterized by a overlapping and coalescing low shields with intervening tube-fed flows The

low eruption rates and intermittent nature of eruptions favors the construction of low shields and the development of channelized and tube-fed flows. Plains volcanism eruption rates are lower than for flood volcanism.The bulk of the volcanics were probably erupted from linear fissures, which may correspond to the present location of Cerberus Rupes. The eruptive fissures were probably relatively narrow; for example the lunar mare fissures are probably 10-25 m wide (Schaber et al., 1976). Typically, in both lunar and terrestrial flood basalt provinces the fissure vents are hidden.

A fluvial origin for the Cerberus Plains, as proposed by Tanaka and Scott (1986) and Tanaka (1986), appears inconsistent with the observed morphology. Although a fluvial episode did occur in the area, it predates the formation of the Cerberus Plains. The absence of a recognized source region for the fluid (presumably water); the absence of a recognized sink; and the burial of channel floors and the channels themselves by the Cerberus Plains are not consistent with a fluvial origin. Channels cut into the knobby terrane can not be traced to the southwest into their source region, nor to the northeast into the debouchment area; presumably they are overlain by the younger plains. In western Cerberus Plains, narrow channels (a few kilometers wide) are cut into exposures of older plains. However, these channels are traceable only for short distances and only on the older plains; the channels abruptly end at the contact with the Cerberus Plains.

The interpretation that Cerberus Plains results from flood plains style volcanism late in martian history carries implications for martian thermal history and volcanic evolution on a global scale. Although central construct volcanism (e.g., Olympus Mons) has long been recognized as occurring late in time, flood volcanism has not. Flood volcanism in the period <700 Ma indicates that, at least in the Elysium region, sufficient heat remained to generate large quantities of lava having low viscosity and erupted at high rates. Flood volcanism has been suggested as the origin of the ridged plains units (e.g., Lunae Planum, Solis and Sinai Planum). This type of volcanic activity generally occurred early, and in Tharsis the style of volcanism evolved from flood eruptions into centralized eruptions which built the large Tharsis Montes and Olympus Mons shields. Volcanism in the Elysium region seems to have followed a similar trend from flood eruptions to central construct building. But, the Cerberus Plains indicate that the volcanic style returned to flood eruption again after central constructional volcanism had ended.

REFERENCES: Carr, M., and Clow, G. (1981) *Icarus*, **48**, 91-117. Greeley, R. (1976) *Proc. 7th Lunar Planet. Sci. Conf.*, 2747-2759. Greeley, R. (1982) *J. Geophys. Res.*, **87**, 2705-2712. Greeley, R. and Guest, J. E. (1987) U. S. Geological Survey Miscellaneous Investigation Series Map I-1802B. Schaber, G. G., (1980) *Icarus*, **42**, 159-184. Schaber, G. G., Boyce, J. M., and Moore, H. J. (1976) *Proc. 7th Lunar Planet. Sci. Conf.*, 2783-2800. Scott, D. H., and Tanaka, K. L. (1986) U. S. Geological Survey Miscellaneous Investigation Series Map I-1802A. Tanaka, K. L. (1986) *Proc. 17th Lunar Planet. Sci. Conf., Part I, J. Geophys. Res.*, **91**, E139-E158. Tanaka, K. L., and Scott, D. H. (1986) *Abstracts, 17th Lunar Planet. Sci. Conf.*, 865-866.

FORMATION OF RHYOLITIC RIDGES ON MARTIAN BASALTS. T.K. Porter and P.H. Schultz, Dept. of Geology, Brown University, Providence, RI 02912

Introduction: Martian lava flows centered at approximately 3° N, 140° W are characterized by steep, thick flow fronts, large areal extents, and distinctive textures. These flows are strikingly different from other martian flows (see Figures 1a and b). The texture has been interpreted as festoon or pressure ridges [1] like those on terrestrial pahoehoe basalts - yet the martian ridges are the same scale as those on terrestrial rhyolite flows [2]. As discussed in [3], the height and spacing of the ridges is controlled by the thickness of the chilled upper margin of the flow and the viscosity ratio (the viscosity of the chilled crust of the flow vs. the viscosity of the flow interior). A thick crust and high viscosity ratio are conditions that favor the formation of high ridges with long wavelengths. Here, analytical modeling and preliminary experimental results suggest that the martian flows could not have developed a crust sufficiently thick to form the observed ridges if the flows were emplaced subaereally, and that instead the flows may have been emplaced under a unit of ice-rich dust.

Viscosities of Martian Flows: We used high resolution Viking Orbiter photographs to determine an average ridge spacing of 175.5m and an average ridge height of 13.9m. These dimensions are one to two orders of magnitude greater than the ridge dimensions of typical terrestrial basalts and are similar to ridge dimensions found on terrestrial rhyolites ([2], [3]). They are unlike any lunar basalts. We inserted the values found in Table 1 into analytical models ([1], [2], [3]) to obtain viscosities (Table 2). The lower viscosities are high for terrestrial basalts ([1], [4]) while the larger viscosity values approach the terrestrial rhyolite viscosities [2]. But these flows are undoubtedly basaltic: observed lava channels and abundant evidence for tube-fed flow are distinctive characteristics of basalts [5]. The long flow distances (up to 6000km^2) over low gradients combined with the large areal extent of these flows (1000 to 4000km^2) indicate a low-viscosity lava; paradoxically, the steep flow fronts, ridge dimensions and analytical models suggest a high-viscosity lava [6]. Recent experiments with molten carbowax [7] indicate that ridge creation is favored if the flow rate is "sufficiently slow" and the ambient temperature is "sufficiently low." Therefore, forming a thick chilled crust on the martian lavas may impart a high-viscosity appearance to a low-viscosity flow. A low-viscosity lava can form steep, thick flow fronts if the flow cools quickly enough. Icelandic table mountains, for example, are basalts that erupted subglacially, producing steep-sided, flat-topped mountains ([8], [9]). The slopes of the steeper terrestrial table mountains are approximately 32° [8]. For comparison, we derive flow front slopes of about 36° for the martian lavas (see Fig. 1a.), in contrast to the thickest lunar flows which have flow front slopes of about 14°.

Apparent High Viscosity from Low Viscosity Flows: The high-viscosity appearance of the martian flows might be produced by quickly and efficiently cooling the surface of a low-viscosity flow. Rapid cooling of the flow surface could be achieved by emplacing the flow under a material with high heat capacity and high thermal diffusivity This would create a thick chilled crust and, by exerting a downward force, could increase the drag component on the surface; both conditions enhance ridge formation. Many of the observed flows are surrounded by easily eroded deposits and the surfaces of some flows exhibit heavily eroded impact craters indicating differential removal of a friable surface deposit at least 300m thick. Models of the rate of cooling of terrestrial lava flows [7] permit calculating the thermal diffusivity of the boundary environment for the martian flows. Using this model and the parameters in Table 1, and then solving for the thermal diffusivity yields a value that is a hundred times too high for air, water or ice and is a hundred times too low for most rock. An ice-rich dust may produce the appropriate thermal diffusivity.

Preliminary experimental results suggest that overburden pressure on the lava flow may play an important role in creating the observed textures. By simulating lava flows with molten carbowax, we have found that efficient cooling alone is not enough to produce the large-scale ridge texture and the steep flow fronts at this scale. To determine the first-order trends of ridge formation, we have emplaced the molten wax in varying conditions such as: subaeral with ambient temperatures varying from -2° to 20° C; under water varying from 0° to 25° C; under powdered dry ice, snow and foam to simulate a material with high heat capacity but low thermal diffusivity. Cooling the wax flows with dry ice or 0°C air is not as efficient at producing large ridges and steep flow fronts as is cooling the flows with ice water - even though the thickness of the chilled margin is roughly the same in all cases.

Conclusion: The observed martian flows have large areal extents and flow lengths, indicating a fluid basalt; the same flows paradoxically have steep flow fronts and a long ridge wavelength, indicating a highly viscous (almost rhyolitic) lava. A low-viscosity basalt may resemble a high-viscosity lava if the flow cools quickly and efficiently enough to produce a thick surface crust, and if thereby exerting drag force on the crust once formed. Preliminary experimental results suggest that overburden pressures also may be important to ridge formation. If emplaced under a mantle of ice-rich dust, then the martian flows could have cooled quickly and have been sujected to sufficient overburdon pressure

References: [1] Theilig and Greeley (1986) *Proc. LPSC XVII.* [2] Fink (1980) *Geology*, **8**. [3] Fink and Fletcher (1978) *Jour. of Volc. and Geotherm. Res.*, **4**. [4] *Basaltic Volcanism Study Project* (1981). [5] Greeley (1980)

Volcanic Features of Hawaii. [6] *Hawaiian Planetary Conference.* (1974). [7] Fink and Griffiths (1989) *LPSC XX.* Abs. [8] Allen (1979) *Jour. Geoph. Res.* [9] Hodges and Moore (1979) *Jour. Geoph. Res.*, 84.

Parameter	Number of Samples	Avg. Value
Ridge spacing	1840	175.5m
Ridge height	8	13.9m
Flow thickness	16	62.5m
Flow front slope	8	36°

Table 1. Parameters obtained using high-resolution VO photographs.

Model	Viscosity in Pa-s	
	Interior	Exterior
Fink and Fletcher (1978)	$5.4 * 10^4$ - $8.7 * 10^6$	$3.4 * 10^5$ - $5.5 * 10^8$
Fink (1980)	$1.5 * 10^6$ - $2.3 * 10^8$	$9.7 * 10^6$ - $1.5 * 10^9$
Theilig and Greeley (1986)	$1.4 * 10^7$ - $2.3 * 10^9$	$1.5 * 10^8$ - $2.5 * 10^{10}$

Table 2. Viscosities obtained from the parameters in Table 1 and the models in [1], [2] and [3].

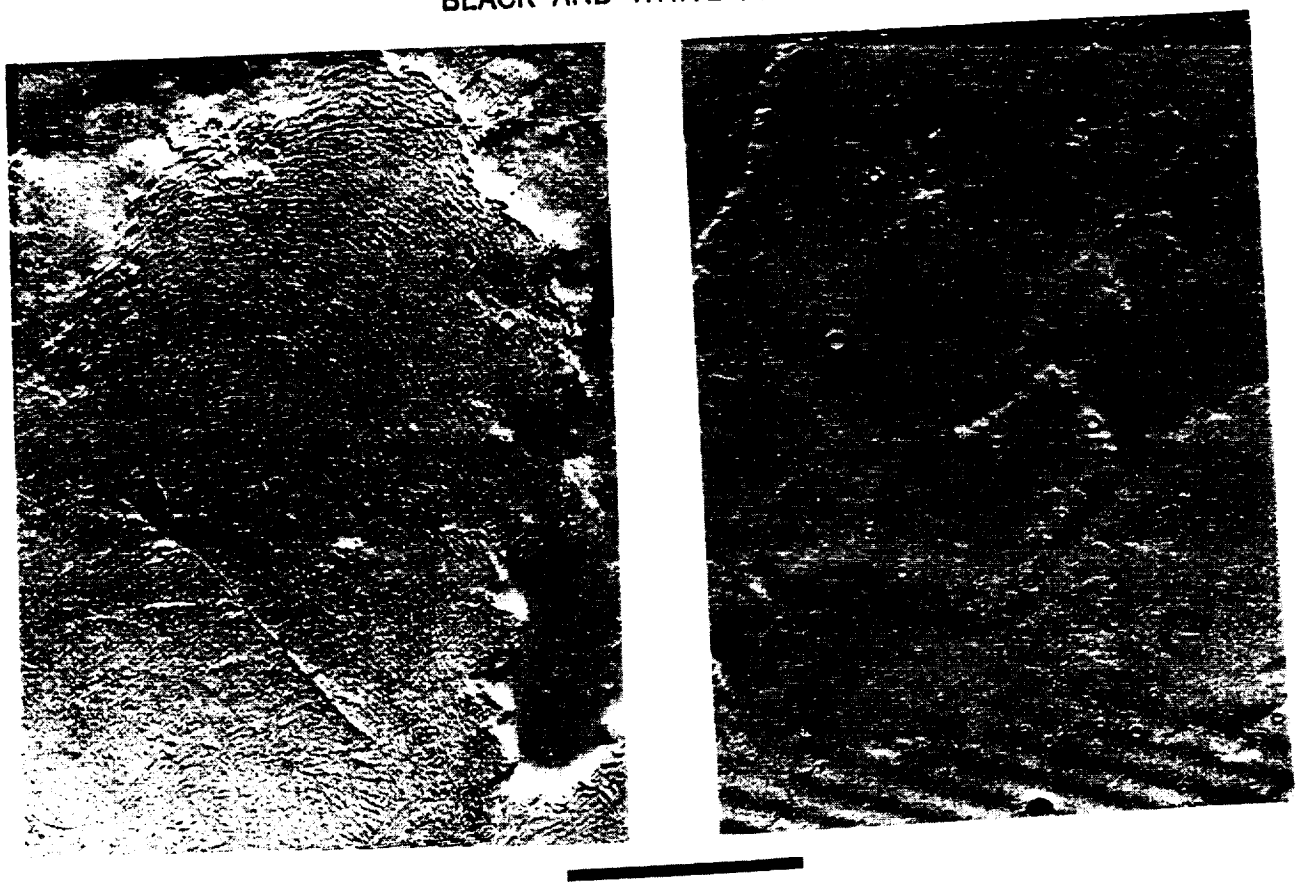

1a. 1b.

Figures 1a. and b. Fig. 1a is a mosaic of 731A03 and 731A04; INA = 75.4°. Note relief and spacing of ridges and steep flow fronts. Fig. 1b. is a portion of 387B13; INA = 72.0°. Here, note flow fronts with less abrupt termini and absence of texture. Scale bar is 10 km for both figures.

MID-INFRARED SPECTRA OF KOMATIITE VS. BASALT

David P. Reyes and Philip R. Christensen, Arizona State University, Tempe,AZ 85287

Komatiite is an ultramafic extrusive containing > 20% weight MgO, and composed mainly of olivine, with lesser pyroxene, and little or no feldspar. On the Earth komatiites were mainly emplaced during the Archean (>2.7 Ga), were erupted at viscosities of 0.1 to 1 Pa, and at temperatures of 1400-1700° C [1,2]. Komatiite was generated at a depth of 150 to 200 km by massive partial melting of the Archean mantle [3]. Their unique character and origin make komatiite excellent indicators of the early composition and development of the Earth's mantle [4]. Komatiites may also be important constituents on Mars [5], and their discovery would provide important constraints on the composition and temperature gradients of the Martian mantle. In addition, determination of the variation in composition of Martian basalts with time can be used to study the evolution of Martian mantle conditions.

The purpose of this study is to determine the mid-infrared spectral properties of komatiite and to compare these to other basalt types. A suite of samples were selected from the Arizona State University petrology collection which were typical of their rock type. The komatiite samples were originally obtained from one of the best preserved komatiite locations in the world, Munro Township, Ontario, Canada [6]. The basalt samples came from various locations and represent a compositional suite from tholeiitic basalt, to alkali basalt, to basaltic andesite. A total of 8 komatiite and 10 basalt samples were analyzed.

Spectra were obtained using a commercial Fourier transform interferometer at a resolution of 4 cm^{-1} in emissive mode. Emission measurements were used because they are appropriate for comparison to remotely gathered planetary data. Samples were heated to 80° C in an oven for 24 hours in order to achieve thermal equilibrium and eliminate thermal gradients. Samples were removed from the oven and analyzed in open air within 10 seconds to minimize thermal gradients due to cooling. Samples were also analyzed on their flat, freshly broken surfaces. Emissivity was calculated relative to a blackbody with > 99 % emissivity and adjustable to > 0.1° C.

The spectra shown in Figures 1 and 2 were selected for presentation because they are typical of all the samples surveyed for their respective groups. Figure 1 shows a comparison of komatiite and olivine. Olivine is a major mineral constituent of komatiite and should, therefore, be discernable in its spectrum. In Figure 1 komatiite show absorption bands at approximately 10.75, 11.25, and 16.5 μm which are due to olivine. Other olivine bands at 9.5, 24.5, 20, and 29 μm are present in the komatiite spectrum but are not clearly discernable, due to overlaping absorption bands of other minerals.

Komatiite spectra from 7 to 30 μm are easily distinguished from basalt spectra as seen in Figure 2. In the 8 to 12 μm region basalts have broad and shallow absorption features. This region results from a concentration of the absorption bands of constituent silicate minerals in basalt, typically olivine, pyroxene, and feldspar. In this same region, komatiite has several narrow, deep bands due primarily to olivine. In the 15 to 30 μm region basalt spectra show a broad region of shallow and indistinct absorption bands. Conversely, in this same region, komatiite show distinctly expressed absorption bands, again due to the predominance of olivine in the komatiite. These spectral features clearly separate ultramafic komatiite from less ultramafic tholeiite basalt and other basalts.

Previous work has shown that there is a detectable and quantifiable shift in the character of spectra in the 8 to 12 μm region as a result of the depolymerization of SiO_2 tetrahedron over large SiO_2 ranges in igneous rocks (ie. rhyolite to basalt) [7]. The results discussed here indicate that this distinction is applicable even to small ranges of SiO_2 content such as from basaltic

andesite to tholeiitic basalt. These shifts can be seen as a discernable difference among the basalt spectra in Figure 2, and are consistent with the general shift of the Si-O absorption band to shorter wavelengths with increasing SiO_2 content. This information is significant in that it indicates that subtle lithologic distinctions can be made from remotely sensed data. This capability is particularly important for Mars, where large variations is SiO_2 content may not occur.

In summary, preliminary data show that in the 7 to 30 μm region komatiite is easily distinguished from all other major basalt types, based on the detailed spectral signature of its constituent minerals, particularly olivine. In addition, subtle variations in basalt composition can be detected and related to variations in bulk rock composition and mineralogy. Future work will focus on a detailed interpretation of the mid-infrared spectra to identify mineral components in all of the basalt samples and quantify the composition variations apparent in Figure 2. These results will be directly applicable to Mars following the receipt of Mars Observer Thermal Emission Spectrometer (TES) data, which will acquire spectra from 6.25 to 50 μm at a spectral resolution comparable to the spectra illustrated in Figures 1 and 2.

References [1] Huppert, H.E., Sparks, S.J., Turner, J.S., and Arndt, N.T., (3/1984), Nature, V. 309, pp.19-22. [2] Arndt, N.T., Francis, D., and Hynes, A.J., (1979), Canadian Mineralogist, V. 17, pp. 147-163. [3] Takahashi, E. and Scarfe, C.M. (6/1985), Nature, V. 315, pp.566-568. [4] Jahn, B.M. and Gruau, G., (1989), LPI Tech Rpt 89-05, LPI,Houston, pp.47-49. [5] Burns, R.G. and Fisher, D.S., (1989), LPI Tech Rpt 89-04, LPI, Houston, pp.20-22. [6] Pyke, D.R., Naldrett, A.J., and Eckstrand, O.R., (3/1973), GSA Bulletin, V. 84, pp 955-978. [7] Walter, L.S. and Salisbury, J.W., (7/1989), JGR, V. 94, N. B7, pp. 9203-9213.

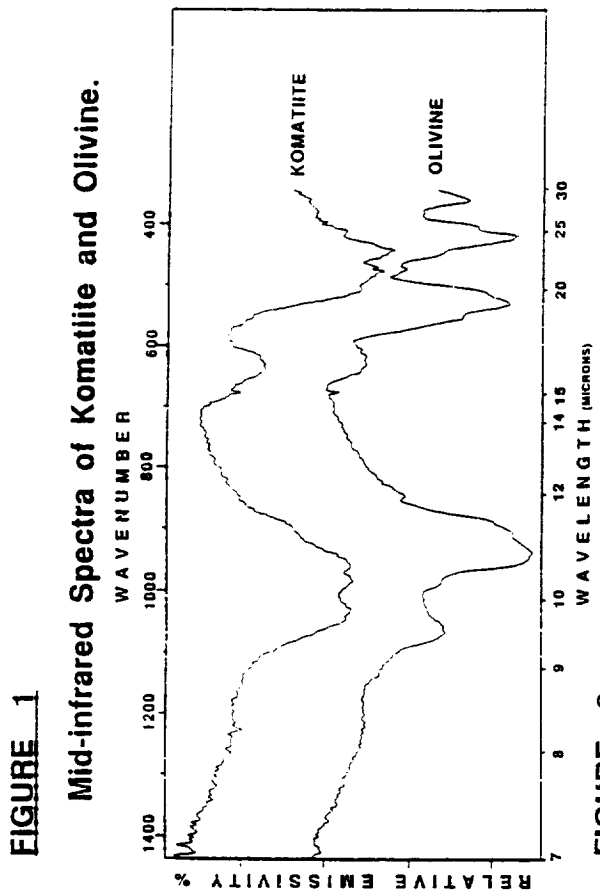

FIGURE 1

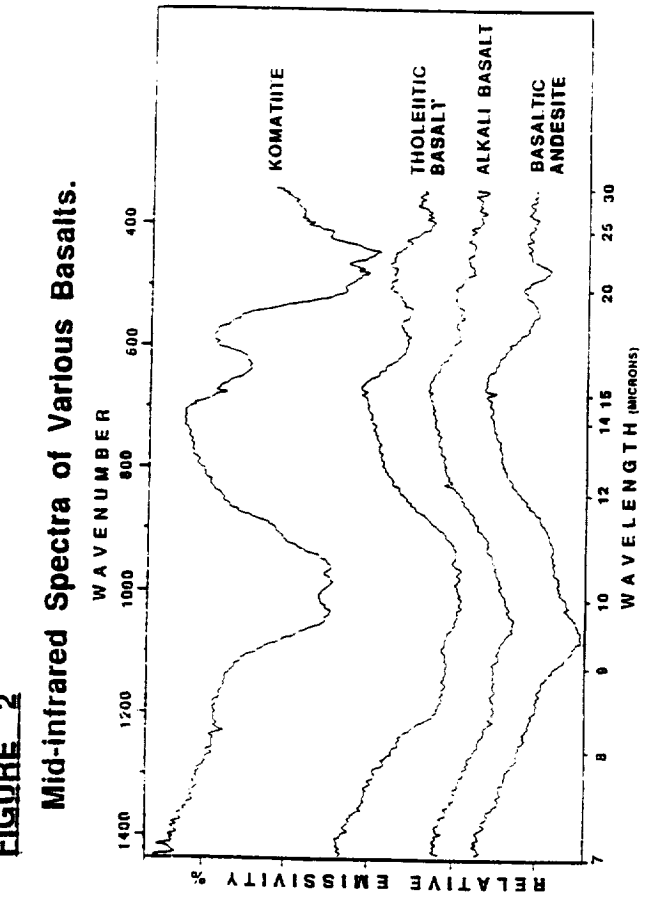

FIGURE 2

THE HIGHLAND-LOWLAND BOUNDARY FORMED ON MARS BETWEEN THE LATE NOACHIAN AND THE EARLY HESPERIAN; Cordula Robinson, ULO Planetary Image Centre, 33-35 Daws Lane, London, NW7 4SD.

The Martian elevation difference has been considered an ancient, stable feature originating early in martian history (3,4,5). Stratigraphical mapping suggests this conventional view needs revision. Further support comes from gravitational data (1) and structural evidence (2).

Detailed stratigraphical mapping provides three pieces of evidence that place constraints on the age of formation of the highland-lowland boundary.

First the plateau material shows volume loss at boundary regions where it acquires a "mesa and butte" form. The confinement to boundary regions suggests volume loss is a consequence of formation of the elevation difference. The volume loss postdates the Middle to Late Noachian plateau material putting a lower limit on the age of boundary formation. Conversely, the "mesa and butte" form is not found in material younger than the plateau material putting an upper limit on the age of boundary formation.

Second the Isidis Basin - formed during the period of bombardment - straddles the boundary. The absence of the north-eastern rim of Isidis implies that the elevation difference came about subsequently.

Finally the absence of large subsurface "ghost" craters in the scarp regions of the boundary, indicates that the early cratering record was obliterated here by destruction and breakage of the palaeosurface.

This work supplements that of McGill (1). He presents new evidence on the age of formation of the highland-lowland boundary, based on detailed analysis of the Viking LOS gravity data. This suggests a weak negative anomaly associated with the boundary region, implying it is not yet fully compensated, as would be expected if it had formed immediately after accretion. McGill supports his proposal with structural data (2) arguing that the boundary in the Eastern Hemisphere was formed as a discrete structural event between Late Noachian and Early Hesperian times. He also proposes that the elevation difference formed in association with the aeolian, fluvial and volcanic resurfacing rates that peaked at these times (6).

Thus, it appears that the elevation difference was attained in a geologically short time interval between the Late Noachian to Early Hesperian; later adjustments are relatively slight. The results suggest that the martian dichotomy stems from endogenic processes and hence mantle differentiation must be a fundamental process in the history of Mars.

References:

(1) McGill G.E. (1988) LPI Tech. Rpt. 89-04 pp.59-61.
(2) Maxwell T.A. and McGill G.E. (1988) Proc.LPSC 18 pp.701-711.
(3) Wise D.U. et al (1979) JGR 84 pp.7934-7939.
(4) Wilhelms D.E. and Squyres S.W. (1984) Nature 309 pp.138-140.
(5) Frey H. and Schultz R.A. (1988) Geophys. Res Letts. 15 pp.229-232.
(6) Tanaka K.L. et al. (1987) Proc.LPSC 18 pp.665-678.

PRECISE TOPOGRAPHIC MEASUREMENTS OF APOLLINARIS AND TYRRHENA PATERAE, MARS.

Mark S. Robinson, Hawaii Institute of Geophysics, Planetary Geosciences Division, 2525 Correa Road, Honolulu Hawaii, 96822.

Introduction

Topographic measurements have been used to classify and interpret both terrestrial and martian volcanoes in previous studies [1-6]. However, the topography for most martian volcanos is not constrained to a high precision, making classification and interpretation difficult. To derive precise topography for martian volcanoes I have taken shadow measurements and photoclinometric profiles from Apollinaris and Tyrrhena Patera. Apollinaris Patera has been classified as a shield, while Tyrrhena Patera is classified as a highland patera [1]. Although the two volcanos have been classified differently (according to morphology) they share some gross morphologic and geographic features. Both occur in the southern hemisphere away from the two major martian volcanic provinces - Tharsis and Elysium, and both are roughly 200 km across. The major difference between the two is their relief, Apollinaris Patera is approximately 5 km high while Tyrrhena Patera is lower (~ 2 km). Based on its low relief and style of erosion previous workers have interpreted Tyrrhena Patera to be the result of dominantly pyroclastic activity [1], resulting in an ash shield, while Apollinaris Patera has been interpreted to be built from effusive activity [1], although others [7] have classified Apollinaris as a composite (pyroclastic + effusive).

Methods

Shadow measurements can provide very precise height determinations if the following conditions are met; 1) low sun angle above the horizon, 2) pixel size is much smaller than the size of the feature being measured and 3) relatively distortion free viewing geometry (low emission angle). Fortunately, Viking images exist of Apollinaris and Tyrrhena Paterae that meet these criteria. To determine accurate shadow lengths actual DN values from calibrated Viking images [8] were observed. Measuring shadows from photographic prints can be difficult due to contrast stretches that can make determination of the shadow edge inaccurate. Error reported on the shadow measurements is determined from the assumption that the top and bottom of the shadow can each be located to within 3/4 pixel accuracy (total error, 1 1/2 pixels).
Photoclinometry [8,9] was employed to measure flank slopes of Apollinaris Patera and Tyrrhena Patera. For the method to determine an accurate slope, all changes in brightness must be the result of a change in slope, not albedo. Inspection of Viking images from multiple passes (in multiple wavelengths) over Apollinaris Patera (8 orbits) and Tyrrhena Patera (5 orbits) revealed no gross change in brightness other than that due to change in slope (across the measured profile). Current work includes the reduction and analysis of Viking color data from 4 different orbits to determine any subtle albedo changes that may be affecting the photoclinometry. Estimation of a flat field (DN value of a flat surface) was done by examining the DN values of caldera floors and at breaks in slope (caldera rim, impact crater rim). Incorrect determination of the flat field introduces serious error to a given profile. However the validity of the flat field can be checked by taking a profile across a fresh bowl-shaped crater, or by comparing photoclinometricly derived heights with shadow measurements. If the profile across a fresh bowl shape crater determines that the two rims are of the same height and shadow measurements correspond to profile height, then a high confidence level can be put on the flat field value. These checking procedures were carried out whenever possible.

Results

Apollinaris Patera: Shadow measurements (635A57 INA=79.5^{o} , Res= 250 m/pix) indicate a minimum relief of 5100 ± 90 m for the west flank of the volcano (Fig. 1). The slope of the volcano under the shadow must be greater than the angle of the sun above the horizon, 10.5^{o}. Shadow measurements were also taken of the caldera wall, determining a height of 770 ± 90 m. Photoclinometric profiles show a distinct break in slope approximately 12 km from the summit plateau. The lower flanks have a minimum slope of 3.7^{o} ± 0.4^{o} while the upper regions have a minimum slope of 5.7^{o} ± 0.6^{o} (actual slopes are greater due to the oblique angle of the profile to the topographic slope). This change in slope may reflect a change in eruptive style (effusion rate, chemistry, volatile content). **Tyrrhena Patera:** Both high and moderate resolution low-sun angle images of the Tyrrhena Patera region were used to determine flank slopes and caldera scarp heights. Shadow measurements from orbit 445A (INA=68^{o}, res=60 m/pix) indicate that the caldera scarp (Fig. 1) is typically 400 m high, with the maximum relief being 470 ± 35 m. Photoclinometric profiles (image 087A14, res=230 m/pix) indicate that the maximum slope on the measured flank is 3.6^{o} ± 0.5^{o}. The accuracy of the photoclinometric profiles was checked using shadow measurements from the high resolution images.

Conclusions

The lower slopes of Apollinaris Patera are comparable to the slopes measured for Tyrrhena Patera suggesting a similar evolution. The break in slope on Apollinaris may reflect a change in the style of eruption from an early stage activity similar to Tyrrhena Patera to a later stage, effusive episode. The basal scarp that skirts Apollinaris may reflect the interface between a relatively unconsolidated, and easily eroded, base (pyroclastic) and an overlying resistant cap (effusive). This model is similar to that proposed by Mouginis-Mark et al [10] for the evolution of Alba Patera. The measured depths of the caldera will be used as a constraint on the geometry of the magma chamber underlying each volcano. Future work will include similar measurements for other martian volcanos to allow for a global interpretation, at a greater precision than previously possible, of volcanic processes on Mars.

References

[1] Greeley, R. and Spudis, P.D. (1981) *Revs. Geophys. and Spa. Phys.* vol. 19 no. 1, pp 13-41. [2] Blasius, K.R. and Cutts, J.A. (1981) *Icarus* 45, pp 87-112. [3] Pike, R.J. (1978) *Proc. LPSC 9th*, pp 3239-3273. [4] Pike, R.J. et al (1980) *NASA TM-81776*, pp. 192-194. [5] Davis, P.A. and Tanaka, K.L. (1987) *MEVTV Workshop on the Nature and Composition of Surface Units on Mars*, pp 49-50. [6] Wu, S.S.C. (1979) *JGR* vol 84 no B14, pp 7955-7959. [7] Plescia, J B. and Saunders, R.S. (1979), *Proc. LPSC 10th*, pp 2841-2859. [8] USGS Astrogeology (1987), *Planetary Image and Cartography System Manual* [9] Davis P. (1984) *JGR* vol 98 no B11, pp 9449-9457. [10] Mouginis-Mark, P.J. et al (1988) *Bull. of Vol.* 50, pp 361-379.

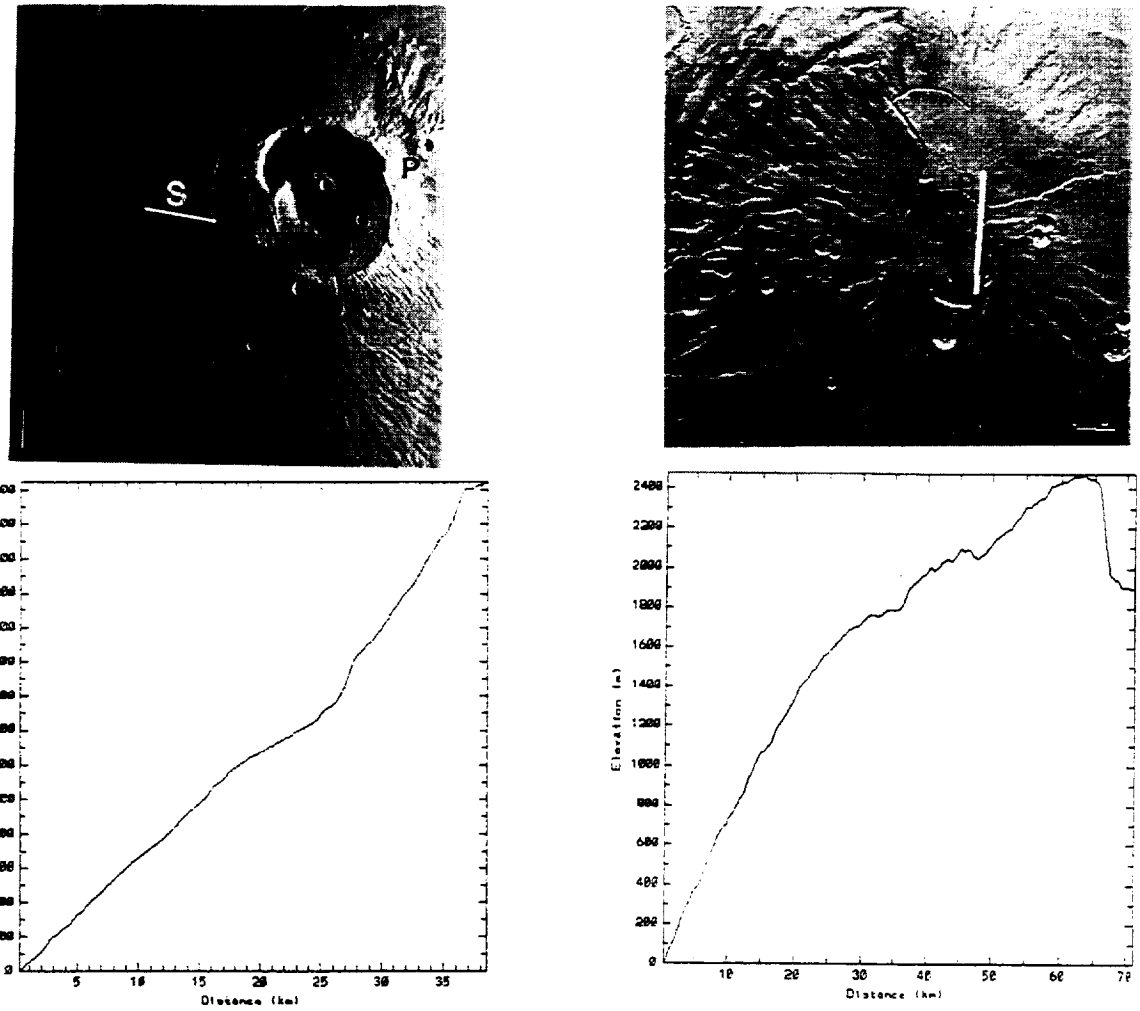

Figure 1. UL - Apollinaris Patera, Viking 635A57 INA=79.5 res=250 m/pix, P indicates photoclinometric profile plotted at LL, S indicates shadow measure of edifice height - 5100 m, scale bar = 50 km. UR - Tyrrhena Patera, Viking 087A14 INA=67°, res=230 m/pix, P indicates photoclinometric profile plotted at LR, scale bar = 46 km.

SINUOUS RIDGES OF THE SOUTH POLAR REGION, MARS: POSSIBLE ORIGINS;

S.W. Ruff and Ronald Greeley, Department of Geology, Arizona State University.

Ridges with sinuous, dendritic, and braided morphologies have been identified in the Dorsa Argentea region near the martian south pole and in the Argyre Planitia (Figure 1). They are < 1 km wide, 100-200 m high, and lengths can exceed 200 km. In planform they vary from relatively straight, solitary features to complex, dendritic and braided patterns. In the Dorsa Argentea region, bifurcating and intersecting relationships of ridges give rise to the dendritic patterns. Some ridges are observed to cross medium-sized, partly buried craters while others cross over each other. Ridge intersections are of two types: merging/bifurcating and overlapping. The first type occurs at most Y-junctions where a single ridge bifurcates or two ridges merge into one. Overlapping intersections occur at X-junctions, the result of an apparent intersection of two ridges at different elevations to each other. The overlapping intersections appear to arise when stratigraphically separated ridges are exhumed, giving the appearance of an intersection. The origin of these ridges remains enigmatic and only two brief interpretations have been proposed, eskers (1) and unusual lava-flow features (2). Other possibilities include linear dunes, inverted topography, and clastic dikes.

Howard (1) proposed a fluvial origin by basal melting of ground ice to account for the dendritic and braided characteristics of the ridges. This model suggests that the ridges are eskers, the depositional product of meltwater channels within ice. Terrestrial eskers have similar morphological characteristics which compare favorably to those of the martian ridges. In planform eskers are often braided as well as dendritic features which are a few to 100 m high, up to 6 km wide, and several meters to 400 km long (with breaks) (3). The difficulty with this interpretation is that it requires the presence of large quantities of ice which, on Earth, produce a host of associated glacial landforms. These are not readily apparent in the region where ridges occur.

Tanaka and Scott (2) offered a brief interpretation of the ridges as part of their mapping of the polar regions. They suggested that the ridges could be an unusual lava-flow feature. Known ridge forming features associated with lava flows include, among others, basaltic pressure ridges (e.g., 4), wrinkle ridges (e.g., 5), and flow lobes. However, none of these have morphologies which can explain the forms seen in the martian sinuous ridges. An as yet unexplained and unobserved style of lava flow must be proposed then to account for the ridges.

Another possibility, suggested by Malin (personal communication), proposes that the ridges are dunes. Some linear dunes in Australia bare a striking resemblance to the martian ridges. Australian dunes can be sinuous, bifurcating, and irregular in their occurrence (6). Some parts of these dunes have a braided appearance. They are several meters to 1 km wide and up to 190 km long (7). A dune interpretation for the martian ridges is supported by the fact that aeolian processes on Mars are well documented (e.g.,8) and the adjacent polar layered deposits could represent a ready supply of sediment which could be reworked into dunes. The difficulty with this interpretation is that linear dunes on Earth do not have such complex intersecting and bifurcating patterns as the martian ridges.

An alternative suggestion by Howard (1) includes the possibility of inverted topography to explain the ridges. He discarded this idea due to a lack of favorable morphological comparison to known inverted topography at other martian locales as well as on Earth. But, the preservation of channel deposits produced during fluvial or volcanic activity could, following differential erosion, produce ridge forms. This idea is weakened in the case of the martian ridges by the presence of geometries that are not indicative of flow channels. Namely , many of the ridges have V's which open in opposing directions rather than a single upstream direction.

A final hypothesis that was examined came from Malin (personal communication). He suggested clastic dikes as a possible ridge former. Clastic dikes occur where extraneous material invades a crack within a host rock (9). These features are from 2 cm to 10 m thick and a meter to 15 km long. Perhaps differential erosion could result in a ridge form, but this is not a common attribute of clastic dikes. The relatively small size and lack of topographic relief of terrestrial clastic dikes does not favor them as an analog of the martian ridges.

Additional study is required before making final conclusions. Many of the ridges mapped by Tanaka and Scott (2) have not been inspected in detail, nor has a planetwide inventory of similar appearing features been made. Finally, a complete study of morphometric features associated with the martian ridges and terrestrial analogs must be undertaken. If thermal inertia and/or spectral data with fine enough resolution are available in ridge areas, information concerning the composition of the ridges could be elucidated and could help to constrain certain hypotheses.

REFERENCES

(1) Howard, A.D. 1981. Etched plains and braided ridges of the south polar region of Mars: Features produced by melting of ground ice? *Reports of Planetary Geology Program-1981*, NASA TM 84211, 286-289.

(2) Tanaka, K.L. and Scott, D.H. 1987. Geologic map of the polar regions of Mars. U.S. Geol. Surv. *Misc. Invest. Series*, Map I-1802-C 1:15,000,000.

(3) Price, R.J. 1973. *Glacial and Fluvioglacial Landforms*, Hafner Publishing Co., New York, 242 pp.
(4) Theilig, E.E. 1986. Formation of pressure ridges and emplacement of compound basaltic lava flows. PhD thesis, Arizona State University, Tempe.
(5) Maxwell ,T.A, El-Bas, R., and Ward, S.H. 1975. Distribution, morphology, and origin of ridges and arches in Mare Serenitatis. *Geol Soc. Am. Bull.*, **86**, 1273-1278.
(6) Mabbutt, J.A. and Sullivan, M.F. 1968. The formation of longitudinal dunes: evidence from the Simpson Desert. *Austr. Geogr.*, **10**, 483-487.
(7) Breed, C.S. and Grow, T. 1979. Morphology and distribution of dunes in sand seas by remote sensing. In *A Study of Global Sand Seas*, E.D. Mckee, editor. U.S Geol. Surv. Prof. Paper 1052, 253-302.
(8) Greeley, Ronald, Leach, R.N., Williams, S.H., White, B.R., pollack, J.B., Krinsley, D.H., and Marshall, J.R. 1982. Rate of wind abrasion on Mars. *Journ. Geophys. Rev.*, **87**, 10,009-10,024.
(9) Pettijohn, F.J. 1975. *Sedimentary Rocks*. Harper and Row, Publishers, 628 pp.

Figure 1. *Viking photomosaic showing sinuous ridges in Dorsa Argentea.*